J. Fluid Mech. (1983), *vol.* 128, *pp.* 181–198
Printed in Great Britain

Flow-acoustic interaction near a flexible wall

By A. P. DOWLING
Department of Engineering, University of Cambridge, Cambridge CB2 1PZ

(Received 15 May 1982)

The Lighthill theory has been extended so that it may be used to determine the flow noise induced by a turbulent boundary layer over a plane homogeneous flexible surface. The influence of the surface properties and the mean flow on the sound generated is brought out explicitly through the use of a Green function. It is found that there is an analogy between the sound generated by turbulence and equivalent sources placed between a surface with the same compliance as the physical surface and a hypothetical vortex sheet positioned at the outer edge of the boundary layer. This analogy is used to determine the spectrum of the surface-pressure fluctuations under statistically stationary turbulence. The form of this wall-pressure spectrum is investigated in detail for three particular types of surface: rigid surfaces, bending plates and sound-absorbent liners.

1. Introduction

A turbulent boundary layer over a flexible surface generates sound. The flexible surface can influence the sound field in two ways: it may just reflect the sound but it could also alter the turbulence. The Lighthill (1952) theory provides an exact way of investigating sound generation by turbulence, and this paper describes an extension of the Lighthill theory to display the effect of the surface properties and the mean flow on the generated sound. It is shown that the sound produced by turbulent sources within a boundary layer may be modelled by quadrupoles placed between a surface with the same compliance as the physical surface and a hypothetical vortex sheet positioned at the outer edge of the boundary layer. The effects of the surface properties and the mean flow are displayed explicitly through the use of a Green function. This is a generalization of the Green functions used by Dowling, Ffowcs Williams & Goldstein (1978) to investigate the interaction between the mean flow and the sound generated by a jet, and by Ffowcs Williams & Purshouse (1981) to determine the incompressible elements of the pressure disturbance generated by turbulence near a hard wall; the case of uniform flow over a compliant wall was considered by Möhring & Rahman (1979). The radiated sound field is finite, and this imposes restraints on our Green function; it must not excite any instabilities of the analogous problem. The Green function is therefore only weakly causal whenever the model problem has instabilities. The analogy contains elements which admit that, when the mean-flow profile is unstable, then in addition to the turbulence-causing fluctuations in the surface and sound, the surface motion and sound waves also affect the turbulence.

This extension of Lighthill's theory is used to determine the spectrum of the pressure fluctuations on the flexible surface. Particular attention is given to those spectral elements with wavelengths long in comparison with the boundary-layer height, and with sonic or supersonic phase velocities. The form of this pressure

spectrum is of interest in both underwater and aeronautical applications. Most of the previous work on wall-pressure spectra has been concerned with the incompressible regime, where spectral elements have low subsonic phase speeds (a review of this work is given by Willmarth 1975; Ross 1976). Ffowcs Williams (1965) was the first to investigate the sonic and supersonic spectral elements which are strongly influenced by compressibility. Ffowcs Williams (1965, 1982) determined the form of the pressure spectrum for the case of uniform flow over a hard surface. He found that the pressure spectrum had a non-integrable singularity for spectral elements with sonic phase speeds. Bergeron (1973) analysed this singularity in greater detail and showed that this non-integrable singularity arose from a two-dimensional form of Olbers' paradox, because the turbulent source region is considered to be of infinite extent and the sound field from each source element does not decrease rapidly enough with distance for the integrated effect to be finite. He demonstrated that when the source region has finite extent L there is still a singularity for spectral elements with sonic phase speeds but that the singularity is integrable; the magnitude of the integral being proportional to $\ln L$. Howe (1979) investigated the effect of viscous stress on the singularity. He found that when viscosity is included the pressure spectrum remains finite, but its maximum value is so large that viscous stress is unlikely to be the dominant controlling mechanism in practice. The aim of the present work is to determine the effects of finite surface impedance and the flow profile on the form of the pressure spectrum, and in particular on the position of its peaks and singularities.

An expression for the low-wavenumber surface-pressure spectrum on an arbitrary surface is derived in §2. This form brings out the dependence on the main flow and the surface properties. It is investigated in detail in §3 for particular surfaces. The first case considered is that of a hard surface. The inclusion of the boundary-layer flow does influence the surface-pressure spectrum. When the flow profile was neglected, Ffowcs Williams found that the pressure spectrum was singular for all spectral components whose phase speed was equal to the sound speed. The inclusion of the boundary layer controls this singularity for all upstream-propagating spectral elements, but enhances the singularity for downstream-propagating elements. For these components the singularity is a double pole, and is stronger than the single pole found by Ffowcs Williams for uniform mean flow. This singularity is due to a 'trapped' mode, which propagates downstream supersonically in the boundary layer and subsonically in the flow outside it. The energy in this mode therefore remains trapped within the boundary layer and only decays slowly with distance from the source.

The next case considered is that of a bending plate with its front surface exposed to the turbulent boundary layer and backed by a void. Both the finite surface impedance and the boundary layer can influence the pressure spectrum. It is found that plates in air are generally sufficiently massive compared with the effective fluid loading to behave like a hard surface. But in underwater applications the fluid loading is greater and the Mach number is low, so that the pressure spectrum is dominated by the surface properties. In this limit V, the speed of flexural waves in the plate *in vacuo*, plays a crucial role in determining the form of the pressure spectrum on the plate. If V is subsonic then the surface has a 'mass-like' response for modes with sonic phase velocity, and in this case the pressure spectrum has a double pole for spectral components whose phase velocity is nearly equal to V, while for elements with sonic phase speeds the pressure spectrum (which was singular in the hard-surface case) remains finite, controlled by the finite surface impedance. The position of the singularity is quite different when V, the flexural wave speed *in vacuo*, is supersonic;

then the plate has a 'spring-like' response for modes with sonic phase speeds, and a singularity occurs in the pressure spectrum for sonic spectral elements. These non-integrable singularities again arise owing to a form of Olbers' paradox because the plate and the turbulence are assumed to be of infinite extent and there is a mode trapped near the surface in which the pressure only decays slowly with distance from the source.

The final case considered is that of a surface covered by sound-absorbent material with an impedance similar to that used in the suppression of fan noise in aircraft engines. Then both the mean flow and the surface parameters affect the pressure spectrum. The damping due to the energy absorbed by the surface ensures that there are no singularities in the surface-pressure spectrum; but the pattern observed in the case of the bending plate is still apparent. For example, the pressure spectrum for spectral elements with sonic phase speeds is larger for a 'spring-like' surface than it is for a surface with a 'mass-like' response. This is because for a spring-like surface only damping prevents the pressure spectrum from being singular for these sonic spectral components, while for a mass-like surface both the finite surface impedance and the damping control the level of the pressure spectrum.

2. Sound generation by turbulence near a flexible wall

The flow over a flexible wall produces sound and turbulence. In our problem the flexible wall is taken to be only linearly disturbed from its rest position C_0 on the plane surface $x_3 = 0$. The impedance is uniform over the whole surface, and the relationship between the surface-pressure disturbance $p-p_0$ and displacement ξ can be conveniently expressed in terms of their Fourier transforms:

$$\overline{p-p_0}(\mathbf{k},\omega) = X(\mathbf{k},\omega)\,\bar{\xi}(\mathbf{k},\omega), \tag{2.1}$$

where $$\overline{p-p_0}(\mathbf{k},\omega) = \int (p-p_0)(x_1,x_2,0,t)\,e^{-i(\omega t+k_1x_1+k_2x_2)}\,dx_1\,dx_2\,dt,$$

and $\bar{\xi}$ is defined in a similar way.

Far from the wall the flow has a mean subsonic velocity $\mathbf{U}$, parallel to the mean wall position. But in the vicinity of the wall the mean flow is brought to rest. In the distant velocity field the sound generation is described by the convected form of Lighthill's acoustic analogy, but near the surface it is more convenient to use the stationary form. To facilitate the use of different equations in the two regions we introduce a control surface S. We choose S to lie outside the region of turbulent flow, and to be initially plane. Subsequently S is convected with the material fluid particles. S divides the fluid into two regions V_0 and V_1, as shown in figure 1. V_0 contains the turbulent flow, while throughout the region V_1 the flow is only linearly disturbed from the mean flow $\mathbf{U}$.

The only disturbances in V_1 are convected acoustic waves, and so

$$\left(\frac{\bar{D}^2}{D\tau^2}-c^2\nabla^2\right)(\rho-\rho_0) = 0 \quad \text{in } V_1, \tag{2.2}$$

where $\bar{D}/D\tau$ is the convected operator $\partial/\partial\tau+\mathbf{U}.\nabla$, and ρ_0, c are the unperturbed values of density and sound speed. We define a Heaviside function $\bar{H}$ to be unity in V_1 and zero elsewhere.

Muliplying (2.2) by $\bar{H}$ and rearranging gives

$$\left(\frac{\bar{D}^2}{D\tau^2}-c^2\nabla^2\right)\bar{H}(\rho-\rho_0) = -\frac{\partial}{\partial y_i}\left\{(p-p_0)\frac{\partial\bar{H}}{\partial y_i}\right\}+\rho_0\frac{\bar{D}}{D\tau}\left\{(v_i-U_i)\frac{\partial\bar{H}}{\partial y_i}\right\}, \tag{2.3}$$

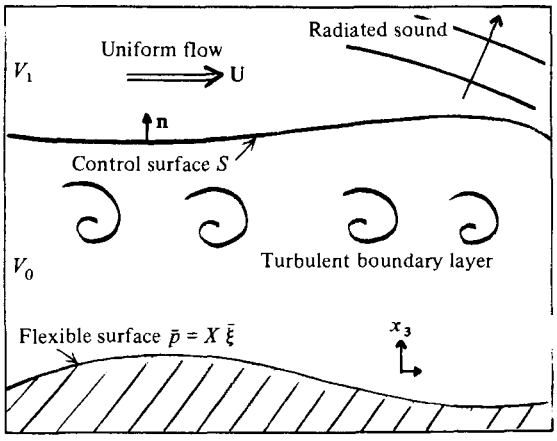

FIGURE 1. The geometry of the turbulent boundary layer.

where $\mathbf{v}$ is the fluid velocity. We can convert this into an integral equation by following the same procedure as that used by Dowling *et al.* (1978). We define a reciprocal Green function G_1 by

$$\left(\frac{\bar{D}^2}{D\tau^2} - c^2\nabla^2\right)G_1 = \delta(\mathbf{x}-\mathbf{y}, t-\tau) \quad \text{in } V_1, \tag{2.4}$$

and G_1 must have incoming behaviour at infinity, in the variables $\mathbf{y}, \tau$. We also insist that G_1 remain finite as $\tau \to -\infty$, and that $G_1 \to 0$ as $\tau \to \infty$. These conditions are not enough to determine G_1 uniquely; G_1 is not completely specified until boundary conditions on S are given.

From the definition of the δ-function we can write

$$\begin{aligned}\overline{H}(\rho-\rho_0)(\mathbf{x}, t) &= \int_\infty \overline{H}(\rho-\rho_0)(\mathbf{y}, \tau)\,\delta(\mathbf{x}-\mathbf{y}, t-\tau)\,d^3\mathbf{y}\,d\tau \\ &= \int_\infty \overline{H}(\rho-\rho_0)\left(\frac{\bar{D}^2}{D\tau^2} - c^2\nabla^2\right)G_1\,d^3\mathbf{y}\,d\tau\end{aligned}$$

from the definition of G_1. After integration by parts

$$\overline{H}(\rho-\rho_0)(\mathbf{x}, t) = \int_\infty G_1\left(\frac{\bar{D}^2}{D\tau^2} - c^2\nabla^2\right)\overline{H}(\rho-\rho_0)\,d^3\mathbf{y}\,d\tau.$$

Terms at infinity vanish because $\overline{H}(\rho-\rho_0)$ has outward-wave behaviour and G_1 has inward-wave behaviour. Hence, from (2.3),

$$\begin{aligned}\overline{H}(\rho-\rho_0)(\mathbf{x}, t) &= \int_\infty \left(-G_1\frac{\partial}{\partial y_i}\left\{(p-p_0)\frac{\partial\overline{H}}{\partial y_i}\right\} + \rho_0 G_1\frac{\bar{D}}{D\tau}\left\{(v_i-U_i)\frac{\partial\overline{H}}{\partial y_i}\right\}\right)d^3\mathbf{y}\,d\tau \\ &= \int_\infty \left(\frac{\partial G_1}{\partial y_i}(p-p_0) - \rho_0\frac{\bar{D}G_1}{D\tau}(v_i-U_i)\right)\frac{\partial\overline{H}}{\partial y_i}d^3\mathbf{y}\,d\tau\end{aligned}$$

after further integration by parts.

A property of the Heaviside function $\overline{H}$ is that

$$\int K(\mathbf{y}, \tau)\frac{\partial\overline{H}}{\partial y_i}d^3\mathbf{y} = \int_S K(\mathbf{y}, \tau)\,n_i\,dS,$$

for any function $K(\mathbf{y},\tau)$. $\mathbf{n}$ is the unit normal to the surface S in the direction shown in figure 1. Hence

$$\overline{H}(\rho-\rho_0)(\mathbf{x},t) = \int_S \left\{\frac{\partial G_1}{\partial y_i}(p-p_0) - \rho_0 \frac{\overline{D}G_1}{D\tau}(v_i-U_i)\right\} n_i \, dS\, d\tau.$$

The surface S is positioned where the flow is only linearly disturbed from the mean flow $\mathbf{U}$, and so these surface terms may be linearized. $n_i(v_i-U_i)$ can be expressed in terms of the surface displacement ξ, and then the integral can be evaluated over the initial position of the surface S_0:

$$\overline{H}(\rho-\rho_0)(\mathbf{x},t) = \int_{S_0} \left\{\frac{\partial G_1}{\partial y_3}(p-p_0) - \rho_0 \frac{\overline{D}G_1}{D\tau}\frac{\overline{D}\xi}{D\tau}\right\} dS\, d\tau.$$

After further rearrangement we obtain

$$\overline{H}(\rho-\rho_0)(\mathbf{x},t) = \int_{S_0} \left\{\frac{\partial G_1}{\partial y_3}(p-p_0) + \rho_0 \frac{\overline{D}^2 G_1}{D\tau^2}\xi\right\} dS\, d\tau. \tag{2.5}$$

This expression describes the radiated sound field. It is, however, impossible to estimate accurately the linear surface terms in (2.5). So as in the jet-noise problem (Dowling *et al.* 1978) we will investigate the region V_0 to try to eliminate these surface terms.

In V_0 the flow is turbulent and generates noise. This generation process can be described by Lighthill's equation

$$\left(\frac{\partial^2}{\partial\tau^2} - c^2\nabla^2\right)(\rho-\rho_0) = \frac{\partial^2 T_{ij}}{\partial y_i \partial y_j}, \tag{2.6}$$

where $T_{ij} = \rho v_i v_j + p_{ij} - (\rho-\rho_0)c^2\delta_{ij}$, and p_{ij} is the compressive stress tensor: $p_{ij} = (p-p_0)\delta_{ij} - e_{ij}$, with e_{ij} being the viscous stress. Equation (2.6) is exact. It results from a combination of the equations of mass and momentum conservation. We introduce H, a Heaviside function which is unity in V_0 and zero elsewhere. All the surfaces bounding V_0 are impenetrable to the fluid, and so multiplying (2.6) by H and rearranging leads to the Ffowcs Williams–Hawkings (1969) equation

$$\left(\frac{\partial^2}{\partial\tau^2} - c^2\nabla^2\right)H(\rho-\rho_0) = \frac{\partial^2 H T_{ij}}{\partial y_i \partial y_j} - \frac{\partial}{\partial y_j}\left(p_{ij}\frac{\partial H}{\partial y_i}\right) + \rho_0 \frac{\partial}{\partial\tau}\left(v_i \frac{\partial H}{\partial y_i}\right). \tag{2.7}$$

We define a reciprocal Green function G_0 by

$$\left(\frac{\partial^2}{\partial\tau^2} - c^2\nabla^2\right)G_0 = \delta(\mathbf{x}-\mathbf{y}, t-\tau), \tag{2.8}$$

and G_0 is bounded as $\tau\to-\infty$ and $G_0\to 0$ as $\tau\to\infty$. These conditions do not completely specify G_0. Then the same procedure that leads from (2.3) and (2.4) to (2.5), with G_0 replacing G_1 and (2.7) in place of (2.3), gives

$$\begin{aligned} H(\rho-\rho_0)(\mathbf{x},t) = {} & \int_{V_0} T_{ij}\frac{\partial^2 G_0}{\partial y_i \partial y_j} d^3\mathbf{y}\, d\tau + \int_{S_0}\left(-(p-p_0)\frac{\partial G_0}{\partial y_3} - \rho_0\frac{\partial^2 G_0}{\partial\tau^2}\xi\right) dS\, d\tau \\ & + \int_{C_0}\left((p-p_0)\frac{\partial G_0}{\partial y_3} - e_{3j}\frac{\partial G_0}{\partial y_j} + \rho_0\frac{\partial^2 G_0}{\partial\tau^2}\xi\right) dy_1 dy_2 d\tau, \end{aligned} \tag{2.9}$$

where C_0 is the initial position of the compliant surface.

Adding (2.5) and (2.9) gives

$$(H+\bar{H})(\rho-\rho_0)(\mathbf{x},t) = \int_{V_0} T_{ij}\frac{\partial^2 G_0}{\partial y_i \partial y_j}d^3\mathbf{y}\,d\tau + \int_{S_0}\left\{(p-p_0)\left(\frac{\partial G_1}{\partial y_3}-\frac{\partial G_0}{\partial y_3}\right)+\rho_0\xi\left(\frac{\bar{D}^2 G_1}{D\tau^2}-\frac{\partial^2 G_0}{\partial\tau^2}\right)\right\}dS\,d\tau + \int_{C_0}\left\{(p-p_0)\frac{\partial G_0}{\partial y_j}-e_{3j}\frac{\partial G_0}{\partial y_j}+\rho_0\frac{\partial^2 G_0}{\partial\tau^2}\xi\right\}dy_1 dy_2 d\tau.$$

We can use the arbitrariness in G_0 and G_1 to eliminate the potentially misleading linear surface terms. If we choose

$$\frac{\partial G_0}{\partial y_3}=\frac{\partial G_1}{\partial y_3},\quad \frac{\partial^2 G_0}{\partial\tau^2}=\frac{\bar{D}^2 G_1}{D\tau^2}\quad \text{on } S_0 \tag{2.10}$$

the surface terms on S_0 vanish. We would like to find other boundary conditions on C_0 to eliminate the surface terms there. By an application of Parseval's theorem we can write

$$\int_{C_0}\left((p-p_0)\frac{\partial G_0}{\partial y_3}+\rho_0\xi\frac{\partial^2 G_0}{\partial\tau^2}\right)dy_1 dy_2 d\tau = \frac{1}{(2\pi)^3}\int\left(\overline{p-p_0}(0,\mathbf{k},\omega)\overline{\frac{\partial G_0}{\partial y_3}}(0,-\mathbf{k},-\omega) - \rho_0\omega^2\bar{\xi}(\mathbf{k},\omega)\bar{G}_0(0,-\mathbf{k},-\omega)\right)dk_1 dk_2 d\omega.$$

This vanishes if

$$\rho_0\omega^2\bar{G}_0(0,\mathbf{k},\omega) = X(-\mathbf{k},-\omega)\overline{\frac{\partial G_0}{\partial y_3}}(0,\mathbf{k},\omega). \tag{2.11}$$

This boundary condition, together with (2.10) and the initial conditions, is enough to determine G_0 and G_1 uniquely. With this choice of G_0, the radiated sound field is given by

$$(H+\bar{H})(\rho-\rho_0)(\mathbf{x},t) = \int_{V_0} T_{ij}\overline{\frac{\partial G_0}{\partial y_i \partial y_j}}d^3\mathbf{y}\,d\tau - \int_{C_0} e_{3j}\frac{\partial G_0}{\partial y_j}dy_1 dy_2 d\tau. \tag{2.12}$$

The sound is generated by the Lighthill quadrupoles within the turbulent boundary layer and by viscous stress on the flexible surface. Purshouse (1978) has obtained a similar expression for the unsteady incompressible pressure fluctuations produced by turbulence near a compliant wall. He chose to apply the rigid-wall condition to his Green function. Our analysis differs from his in that the flow is compressible and also because we apply a more general impedance condition to the Green function and so are able to eliminate the surface-displacement term. Howe's (1979) work has shown that the surface term involving the viscous stress has a negligible effect for the high-Reynolds-number flows of interest.

The effect of the flexible surface and of the variation in mean flow is described by the function G_0. So far G_0 and G_1 have arisen simply as useful functions which eliminate certain potentially misleading surface terms. The reciprocal theorem derived in the appendix shows, however, that

$$G(\mathbf{y},\tau|\mathbf{x},t) = H(\mathbf{y},\tau)\,G_0(\mathbf{y},\tau|\mathbf{x},t)+\bar{H}(\mathbf{y},\tau)\,G_1(\mathbf{y},\tau|\mathbf{x},t)$$

has a simple physical meaning; it is the pressure response at the observer's position $(\mathbf{x},t)$ that would be produced by a point source at $(\mathbf{y},\tau)$ placed between a surface with the same impedance as the physical surface and a hypothetical vortex sheet positioned at the outer edge of the boundary layer.

The equations (2.4), (2.8), with boundary conditions (2.10), (2.11), and the initial conditions, are sufficient to determine G_0 and G_1 uniquely. G_0 can be evaluated by taking Fourier transforms in y_1, y_2 and τ. The method of solution is a straightforward application of the techniques described by Morse & Feshbach (1953) and the details will not be given here. We find that, for an observer position $\mathbf{x}$ on the flexible surface,

$$G_0 = \frac{1}{(2\pi)^3 c^2} \int F_1(y_3, \mathbf{k}, \omega)\, e^{ig_1}\, d^2\mathbf{k}\, d\omega, \tag{2.13}$$

where

$$F_1 = \frac{[(\omega^2\gamma_1 - (\omega + U_1 k_1)^2 \gamma_0)\, e^{i\gamma_0(h-y_3)} - (\omega^2\gamma_1 + (\omega + U_1 k_1)^2 \gamma_0)\, e^{-i\gamma_0(h-y_3)}]\, X^\dagger}{F(\mathbf{k}, \omega)},$$

$$F = (i\gamma_0 X^\dagger + \rho_0\omega^2)(\omega^2\gamma_1 - (\omega + U_1 k_1)^2 \gamma_0)\, e^{i\gamma_0 h} + (i\gamma_0 X^\dagger - \rho_0\omega^2)(\omega^2\gamma_1 + (\omega + U_1 k_1)^2 \gamma_0)\, e^{-i\gamma_0 h},$$

$$g_1 = \omega(\tau - t) + k_\alpha(y_\alpha - x_\alpha).$$

The repeated suffix α is to be summed over 1 and 2 so that

$$k_\alpha(y_\alpha - x_\alpha) = k_1(y_1 - x_1) + k_2(y_2 - x_2).$$

$X^\dagger(\mathbf{k}, \omega)$, the complex conjugate of $X(\mathbf{k}, \omega)$, is equal to $X(-\mathbf{k}, -\omega)$ because $X(\mathbf{k}, \omega)\,(= \overline{(p - p_0)}\,(\mathbf{k}, \omega)/\bar{\xi}(\mathbf{k}, \omega))$ is the ratio between the transforms of two real functions. h is the distance of the control surface S_0 above the flexible surface, and, since S_0 is chosen to lie just outside the region of turbulent flow, h is the boundary-layer height. The coordinate system has been chosen so that the mean position of the compliant surface lies in the plane $y_3 = 0$, and the velocity $\mathbf{U}$ is in the 1-direction; $\mathbf{U} = (U_1, 0, 0)$. Further,

$$\gamma_0 = \left(\frac{\omega^2}{c^2} - k_1^2 - k_2^2\right)^{\frac{1}{2}}, \quad \gamma_1 = \left\{\frac{(\omega + U_1 k_1)^2}{c^2} - k_1^2 - k_2^2\right\}^{\frac{1}{2}}.$$

The root of γ_0 is chosen so that, when real, γ_0 has the sign of ω, and when γ_0 is purely imaginary $\operatorname{Im}\gamma_0$ is positive. The root of γ_1 is chosen in a similar way, with γ_1 having the same sign as $\omega + U_1 k_1$ when real, and $\operatorname{Im}\gamma_1$ positive when γ_1 is purely imaginary. These roots lead to the required inward-wave behaviour in $(\mathbf{y}, \tau)$. The k_1, k_2 contours of integration lie along the real k_1, k_2 axes. The ω-integral is to be evaluated along the weakly causal contour which lies just above the real ω-axis, in order to satisfy the two conditions $G_0 \to 0$ as $\tau \to \infty$, and that G_0 remains bounded as $\tau \to -\infty$. Whenever the analogous problem is unstable, the integrand in (2.13) has a pole in the upper half ω-plane, and G_0 will not be strictly causal. Jones & Morgan (1972) have shown that a strictly causal Green function can excite instabilities, but we have only derived the representation (2.12) for a finite Green function. Our analogy is therefore for a weakly causal Green function and contains elements that admit that the relationship between the turbulence, the surface motion and the sound field is not one of cause and effect. This seems to be entirely reasonable because, when the mean flow is unstable, then, in addition to the turbulence causing the surface motion and sound, the surface motion and the sound field can also produce turbulence. When the boundary-layer–surface combination is stable the integrand in (2.13) has no poles in the upper half ω-plane and our Green function is strictly causal. In most practical situations the analogous problem *will* be unstable, because it is its instability waves that generate the turbulence.

The derivatives of G_0 can easily be evaluated by differentiating (2.13):

$$\frac{\partial^2 G_0}{\partial y_1 \partial y_j} = \frac{1}{(2\pi)^3 c^2} \int F_{ij}(y_3, \mathbf{k}, \omega)\, e^{ig_1}\, d^2\mathbf{k}\, d\omega,$$

where $$F_{\alpha\beta} = -k_\alpha k_\beta F_1 \quad (\alpha \text{ and } \beta \text{ may take the values 1 and 2}), \tag{2.14}$$

$$F_{33} = -\gamma_0^2 F_1, \quad F_{\alpha 3} = F_{3\alpha} = \gamma_0 k_\alpha F_2,$$

with

$$F_2 = \frac{\{(\omega^2\gamma_1 - (\omega + U_1 k_1)^2 \gamma_0)\, e^{i\gamma_0(h-y_3)} + (\omega^2\gamma_1 + (\omega + U_1 k_1)^2 \gamma_0)\, e^{-i\gamma_0(h-y_3)}\}\, X^\dagger}{F(\mathbf{k}, \omega)}.$$

When these forms for the derivatives of G_0 are substituted into (2.12) and the small shear-stress terms are neglected, the representation theorem becomes

$$c^2(\rho - \rho_0)(\mathbf{x}, t) = \frac{1}{(2\pi)^3} \int HT_{ij}(\mathbf{y}, \tau)\, F_{ij}(y_3, \mathbf{k}, \omega)\, e^{ig_1}\, d^2\mathbf{k}\, d\omega\, d^3\mathbf{y}\, d\tau. \tag{2.15}$$

Equation (2.15) gives a formally exact description of the perturbations *on* the flexible surface, and the surface-pressure spectrum can be evaluated from it. The Fourier transform $\bar{p}_s(\mathbf{k}, \omega)$ of the surface-pressure perturbation is

$$\bar{p}_s(\mathbf{k}, \omega) = \int c^2(\rho - \rho_0)(x_1, x_2, 0, t)\, e^{-ik_\alpha x_\alpha - i\omega t}\, d^2\mathbf{x}\, dt,$$

and taking transforms of (2.15) leads to

$$\begin{aligned}\bar{p}_s(\mathbf{k}, \omega) &= \int HT_{ij}(\mathbf{y}, \tau)\, F_{ij}(y_3, -\mathbf{k}, -\omega)\, e^{-i\omega\tau - ik_\alpha y_\alpha}\, d^3\mathbf{y}\, d\tau \\ &= \int \bar{T}_{ij}(y_3, \mathbf{k}, \omega)\, F_{ij}(y_3, -\mathbf{k}, -\omega)\, dy_3,\end{aligned} \tag{2.16}$$

where $\bar{T}_{ij}(y_3, \mathbf{k}, \omega)$ is the Fourier transform of HT_{ij}:

$$\bar{T}_{ij}(y_3, \mathbf{k}, \omega) = \int HT_{ij}(\mathbf{y}, \tau)\, e^{-i\omega\tau - ik_\alpha y_\alpha}\, d^2\mathbf{y}\, d\tau.$$

The surface-pressure spectrum $P(\mathbf{k}, \omega)$ may now be evaluated from

$$\bar{P}(\mathbf{k}, \omega) = \frac{1}{(2\pi)^3} \int \overline{\bar{p}_s(\mathbf{k}, \omega)\, \bar{p}_s(\mathbf{k}', \omega')}\, d^2\mathbf{k}'\, d\omega', \tag{2.17}$$

where the overbar denotes an ensemble average. Equation (2.16) shows that

$$\begin{aligned}&\overline{\bar{p}_s(\mathbf{k}, \omega)\, \bar{p}_s(\mathbf{k}', \omega')} \\ &\quad = \int \overline{\bar{T}_{ij}(y_3, \mathbf{k}, \omega)\, \bar{T}_{kl}(y_3', \mathbf{k}', \omega')}\, F_{ij}(y_3, -\mathbf{k}, -\omega)\, F_{kl}(y_3', -\mathbf{k}', -\omega')\, dy_3\, dy_3'.\end{aligned} \tag{2.18}$$

The ensemble average operates only on $\bar{T}_{ij}\bar{T}_{kl}$ since all the other terms in this expression are deterministic. Rewriting $\bar{T}_{ij}$ in terms of HT_{ij}, we obtain, for statistically stationary turbulence,

$$\overline{\bar{T}_{ij}(y_3, \mathbf{k}, \omega)\, \bar{T}_{kl}(y_3', \mathbf{k}', \omega')} = (2\pi)^3\, \delta(\mathbf{k} + \mathbf{k}')\, \delta(\omega + \omega')\, \mathscr{T}_{ijkl}(y_3, y_3', \mathbf{k}', \omega'), \tag{2.19}$$

where $\mathscr{T}_{ijkl}$ is the Fourier transform of the cross-correlation of the turbulent sources:

$$\mathscr{T}_{ijkl}(y_3, y_3', \mathbf{k}, \omega) = \int \overline{HT_{ij}(\mathbf{y}, \tau)\, HT_{kl}(y_1 + \Delta_1, y_2 + \Delta_2, y_3', \tau + \tau_0)}\, e^{-ik_\alpha \Delta_\alpha - i\omega\tau_0}\, d^2\Delta\, d\tau_0.$$

Combining (2.17)–(2.19) shows that the surface-pressure spectrum is given by

$$P(\mathbf{k},\omega) = \int F_{ij}(y_3,\mathbf{k},\omega)\, F_{kl}(y_3',-\mathbf{k},-\omega)\, \mathscr{T}_{ijkl}(y_3,y_3',\mathbf{k},\omega)\, dy_3 dy_3'.$$

From an inspection of the function F_{ij} defined in (2.14) we see that

$$F_{kl}(y_3',-\mathbf{k},-\omega) = F_{kl}^{\dagger}(y_3',\mathbf{k},\omega),$$

where the dagger denotes the complex conjugate. The surface-pressure spectrum may therefore be rewritten as

$$P(\mathbf{k},\omega) = \int F_{ij}(y_3,\mathbf{k},\omega)\, F_{kl}^{\dagger}(y_3',\mathbf{k},\omega)\, \mathscr{T}_{ijkl}(y_3,y_3',\mathbf{k},\omega)\, dy_3 dy_3'. \tag{2.20}$$

F_{ij} is the function given in (2.14). It depends on the surface compliance, the mean flow velocity and on the thickness of the boundary layer. Equation (2.20) shows that $F_{ij}F_{kl}^{\dagger}$ relates the spectrum of the surface pressure to $\mathscr{T}_{ijkl}$, a spectrum function representing the turbulent sources. This is a useful form because in practice, while we know very little about the structure of the turbulent source terms T_{ij}, we can make some reasonable assumptions about the behaviour of their spectral function $\mathscr{T}_{ijkl}$.

In many of the flows of practical interest the boundary layer is thin in comparison with the wavelength. In this limit F_{ij} simplifies considerably and we can write

$$P(\mathbf{k},\omega) = D_{ij}D_{kl}^{\dagger}\int \mathscr{T}_{ijkl}(y_3,y_3',\mathbf{k},\omega)\, dy_3 dy_3', \tag{2.21}$$

where D_{ij} is the compact limit of F_{ij}:

$$D_{\alpha\beta} = \frac{k_\alpha k_\beta(\omega+U_1k_1)^2X^{\dagger}}{E(\mathbf{k},\omega)} \quad (\alpha,\beta = 1 \text{ or } 2),$$

$$D_{\alpha 3} = D_{3\alpha} = \frac{\omega^2 k_\alpha \gamma_1 X^{\dagger}}{E(\mathbf{k},\omega)}, \quad D_{33} = \frac{\gamma_0^2(\omega+U_1k_1)^2X^{\dagger}}{E(\mathbf{k},\omega)},$$

with

$$E(\mathbf{k},\omega) = i\omega^2\gamma_1 X^{\dagger} - \rho_0\omega^2(\omega+U_1k_1)^2 + \rho_0\omega^4 i\gamma_1 h + (\omega+U_1k_1)^2\gamma_0^2 hX^{\dagger}. \tag{2.22}$$

Terms of order $\omega h/c$ have been neglected in comparison with unity. If the acoustic analogy has been successful in extracting the essential field structure, $\mathscr{T}_{ijkl}$ should contain no subtleties of form and should be independent of compressibility effects. $\mathscr{T}_{ijkl}$ can therefore be estimated on the basis of incompressible flow theory. We will non-dimensionalize the integral in (2.21) and write

$$\int \mathscr{T}_{ijkl}(y_3,y_3',\mathbf{k},\omega)\, dy_3 dy_3' = \rho_0^2 U_1^3 h^5 Q_{ijkl}(h\mathbf{k}, h\omega/U_1),$$

and then the pressure spectrum simplifies to

$$P(\mathbf{k},\omega) = D_{ij}D_{kl}^{\dagger}\rho_0^2 U_1^3 h^5 Q_{ijkl}(h\mathbf{k}, h\omega/U_1). \tag{2.23}$$

The product $D_{ij}D_{kl}^{\dagger}$ describes how the turbulent field Q_{ijkl} radiates sound within the boundary layer over the flexible surface. An investigation of the form of D_{ij} for any particular surface of interest will demonstrate the influence of the surface properties and the mean-flow profile on the pressure spectrum.

3. The wall-pressure spectrum on various surfaces

Equations (2.22) and (2.23) describe the influence of the surface structure and mean-flow profile on the wall-pressure spectrum. In this section the form of the pressure spectrum will be investigated for several simple surfaces. The first case considered is that of a hard surface.

3.1. *A hard surface*

The normal surface displacement always vanishes on a hard surface, and so X is infinite. From (2.23) the pressure spectrum is given by

$$P(\mathbf{k},\omega) = D_{ij} D_{kl}^{\dagger} \rho_0^2 U_1^3 h^5 Q_{ijkl}(h\mathbf{k}, \omega h/U_1), \tag{3.1}$$

where D_{ij} can be evaluated by taking the limit $X \to \infty$ in (2.22):

$$D_{\alpha\beta} = \frac{k_\alpha k_\beta (\omega + U_1 k_1)^2}{E(\mathbf{k},\omega)}, \quad D_{\alpha 3} = D_{3\alpha} = \frac{\omega^2 k_\alpha \gamma_1}{E(\mathbf{k},\omega)}, \quad D_{33} = \frac{\gamma_0^2 (\omega + U_1 k_1)^2}{E(\mathbf{k},\omega)},$$

with

$$E(\mathbf{k},\omega) = i\omega^2 \gamma_1 + (\omega + U_1 k_1)^2 \gamma_0^2 h. \tag{3.2}$$

Figure 2 shows plots of the variation of the functions D_{ij} against non-dimensional wavenumber $k_1 c/\omega$ for a Mach number $M_1 = U_1/c$ of 0·2, and a non-dimensional boundary-layer height $\omega h/c = 0{\cdot}1$. Before describing the detail in the graphs, it is convenient to discuss some analytical results. First, the wall-pressure spectrum simplifies greatly for spectral elements with highly supersonic phase velocities. Then $|\omega| \gg c|\mathbf{k}|$, and D_{33}, the largest term in D_{ij}, is equal to $-i\omega/c$. Hence, from (3.1),

$$P(\mathbf{k},\omega) \sim \left(\frac{\omega h}{c}\right)^2 \rho_0^2 U_1^3 h^3 Q_{3333}.$$

This agrees with the scaling law for highly supersonic spectral components obtained by Ffowcs Williams (1965, 1982). Figure 2 (*b*) illustrates the form of 20 $\log_{10} |cD_{33}/\omega|$. It shows that $\log_{10} |cD_{33}/\omega|$ is very nearly equal to zero for $|ck_1/\omega| < 0{\cdot}5$, i.e.

$$|D_{33}| \sim \frac{\omega}{c} \quad \text{for} \quad \left|\frac{ck_1}{\omega}\right| < 0{\cdot}5,$$

and in fact the 'highly supersonic' limit is attained whenever the phase speed is greater than about $2c$.

If $E(\mathbf{k},\omega)$ has any zeros for real $(\mathbf{k},\omega)$ they will lead to a singularity in the pressure spectrum. It is apparent from an inspection of (3.2) that $E(\mathbf{k},\omega)$ vanishes when γ_1 is imaginary and γ_0 is real. This only happens when k_1 and ω are opposite in sign, i.e. for downstream-propagating modes. For a thin boundary layer the position of these zeros can be found by solving $E(\mathbf{k},\omega) = 0$ iteratively in powers of h. It is convenient to describe the position of these zeros in terms of new variables k and ϕ, where $k_1 = -k\cos\phi$, $k_2 = -k\sin\phi$ and $k(= \mp|\mathbf{k}|)$ has the same sign as ω. Then ω/k is the phase speed of the $(\mathbf{k},\omega)$ spectral element, and ϕ denotes its direction of propagation. $E(\mathbf{k},\omega)$ only vanishes for real $\mathbf{k}$ and ω when $\cos\phi$ is positive, and then the zeros are at

$$k = +\frac{\omega}{c(1 + M_1\cos\phi)} + 2M_1^2\cos^2\phi\,\frac{\omega^3 h^2}{c^3}\frac{(1 + \frac{1}{2}M_1\cos\phi)^2}{(1 + M_1\cos\phi)^8} + O(h^3). \tag{3.3}$$

These are modes which propagate downstream supersonically within the stationary fluid in the boundary layer, but they are just subsonic in the moving stream. $D_{\alpha\beta}$

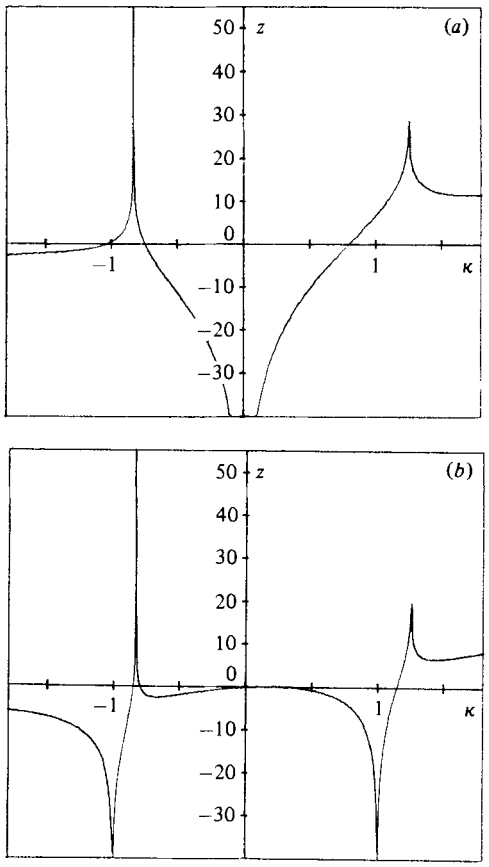

FIGURE 2. Plots of (*a*) $z = 20\log_{10}|cD_{11}/\omega|$, (*b*) $z = 20\log_{10}|cD_{33}/\omega|$ *vs.* non-dimensional wavenumber $\kappa = k_1 c/\omega$ for a hard surface with $k_2 = 0$, $M_1 = 0{\cdot}2$, $\omega h/c = 0{\cdot}1$.

therefore has a simple pole for downstream-propagating spectral elements. In figure 2, $\kappa = k_1 c/\omega$ is negative for downstream-propagating spectral components and positive for the upstream-propagating elements. The curves in figure 2 therefore clearly demonstrate that, D_{ij}, and hence the predicted pressure spectrum, is larger for downstream-propagating modes with sonic phase speeds than it is for upstream propagating modes. Roebuck & Richardson (1981 private communication) have observed this in underwater experiments.

The pressure spectrum involves products $D_{ij}D^{\dagger}_{kl}$, and so a simple pole in D_{ij} corresponds to a double pole in the predicted pressure spectrum. Ffowcs Williams (1965) found that, if the mean-flow profile is neglected, the pressure spectrum has a simple pole for all spectral elements with sonic phase speed. The inclusion of the mean-flow profile controls that singularity for all upstream-propagating modes, but enhances the singularity for modes propagating downstream. Bergeron (1973) and Ffowcs Williams (1982) were able to interpret the singularity found by Ffowcs Williams in terms of a slow decay rate of the sound field with distance R, from a source, because the sound field from each source element decays like R^{-1} and the turbulent source region is assumed to be of infinite extent. They showed that if this region of turbulence is assumed to be of finite size, the pressure spectrum is still singular, but the singularity is integrable. The strength of the integral depends on ln L, where L

is the linear dimension of the turbulent region, so that when L is large the integrated pressure spectrum is still large. A similar explanation can be applied to the case with a mean-flow profile. The zeros of $E(\mathbf{k},\omega)$ given in (3.3) describe downstream-propagating free modes which are supersonic within the slowly moving fluid in the boundary layer but subsonic within the moving fluid outside it. The energy in these modes therefore remains 'trapped' within the boundary layer, i.e. within a disk of height h, and conservation of energy then suggests that downstream of a source the pressure disturbance will only decay like $R^{-\frac{1}{2}}$, while upstream the disturbance will decay more rapidly. This prediction can be confirmed by evaluating the k_1 and k_2 integrals in the expression for G_0 in (2.13) asymptotically for large R. These modes decay more slowly with distance from the source than those in a uniform stream, and account for the stronger singularity in the pressure spectrum under an infinite region of turbulence. For a finite but large patch of turbulence the singularity will be integrable, but the value of the integral will still be large. The effects of finite source size will be discussed in a later paper.

The inclusion of the boundary-layer profile on a hard surface has therefore eliminated the singularity from the predicted hard-wall pressure spectrum for upstream-propagating modes, but enhanced the singularity for downstream-propagating modes.

3.2. *A bending plate*

Admitting that the surface has finite mass per unit area has considerable consequences for the pressure spectrum. Consider a bending plate of thickness d with its front surface exposed to the turbulent boundary layer and backed by a void. For such a plate $X(\mathbf{k},\omega) = m\omega^2 - Bk^4$, where m is the mass of the plate per unit area and $B = Ed^3/12(1-\nu^2)$. E is Young's modulus, and ν Poisson's ratio. Then, from (2.22) and (2.23), the surface-pressure spectrum is given by

$$P(\mathbf{k},\omega) = D_{ij} D_{kl}^{\dagger} \rho_0^2 U_1^3 h^5 Q_{ijkl},$$

where

$$D_{\alpha\beta} = \frac{k_\alpha k_\beta (\omega + U_1 k_1)^2 (m\omega^2 - Bk^4)}{E(\mathbf{k},\omega)},$$

$$D_{\alpha 3} = D_{3\alpha} = \frac{k_\alpha \omega^2 \gamma_1 (m\omega^2 - Bk^4)}{E(\mathbf{k},\omega)}, \tag{3.4}$$

$$D_{33} = \frac{\gamma_0^2 (\omega + U_1 k_1)^2 (m\omega^2 - Bk^4)}{E(\mathbf{k},\omega)},$$

with

$$E(\mathbf{k},\omega) = (i\omega^2\gamma_1 + (\omega + U_1 k_1)^2 \gamma_0^2 h)(m\omega^2 - Bk^4) - \rho_0 \omega^2 (\omega + U_1 k_1)^2 + \rho_0 \omega^4 i\gamma_1 h. \tag{3.5}$$

It is immediately obvious that the pressure spectrum vanishes for spectral elements whose phase speed is equal to $V = (B\omega^2/m)^{\frac{1}{4}}$, the phase speed of flexural waves in the plate *in vacuo*.

There will be a singularity in the pressure spectrum if $E(\mathbf{k},\omega)$ vanishes for real $\mathbf{k}$ and ω. For heavy plates and thin boundary layers the position of any zeros can be found by solving $E(\mathbf{k},\omega) = 0$ iteratively in powers of h and m^{-1}. This procedure shows that $E(\mathbf{k},\omega)$ vanishes for real ω and $\mathbf{k}$ near

$$\frac{\omega}{k} = c(1 + M_1 \cos\phi) \tag{3.6}$$

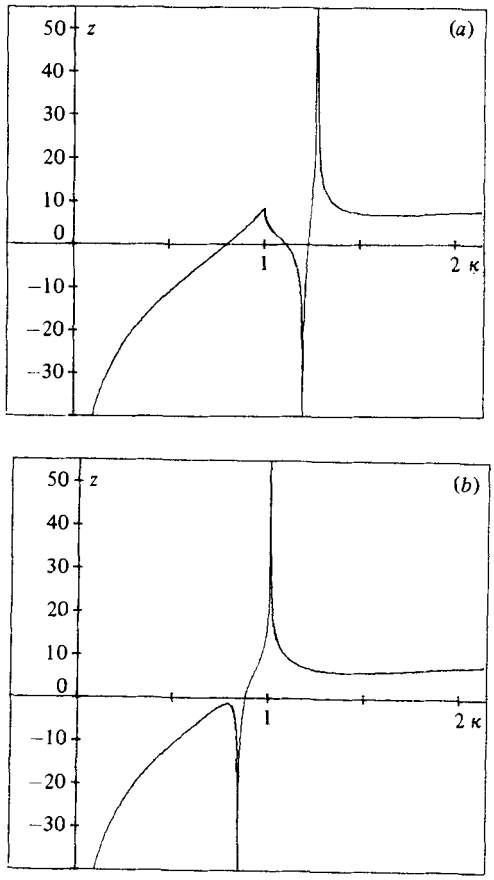

FIGURE 3. Plots of $z = 20\log_{10}|cD_{11}/\omega|$ *vs.* non-dimensional wavenumber $\kappa = k_1 c/\omega$ for a bending plate with $k_2 = 0$, $M_1 = 0$, and (*a*) $m\omega/\rho_0 c = 5$, $N = 0{\cdot}8$, (*b*) $m\omega/\rho_0 c = 10$, $N = 1{\cdot}2$.

if

$$\frac{\rho_0 c^2}{m\omega^2[N^4-(1+M_1\cos\phi)^4]}+2hM_1\cos\phi\frac{(1+\frac{1}{2}M_1\cos\phi)}{(1+M_1\cos\phi)^6}>0, \tag{3.7}$$

where $N = V/c$. $E(\mathbf{k},\omega)$ also has a zero on the real axis near

$$\frac{\omega}{k} = V \quad \text{if} \quad V < 1+M_1\cos\phi. \tag{3.8}$$

The first inequality, (3.7), demonstrates that the relative magnitudes of the fluid-loading factor $\rho_0 c/m\omega$ and the product of the Mach number and non-dimensional boundary-layer height, $M_1\omega h/c$, influence the form of the pressure spectrum. For plates in air the fluid-loading factor is very small, so that the first term in (3.7) is generally negligible in comparison with the second. The inequality then reduces to $\cos\phi > 0$, so that there is a singularity for downstream-propagating spectral elements with nearly sonic phase speeds. This is the same as the hard-surface case. Plates in air are generally sufficiently massive, compared with the effective fluid loading, to behave like a hard surface. But in underwater applications the fluid loading is greater and the Mach number is low, so that the pressure spectrum is dominated by the surface properties. Then the first term in (3.7) is much larger than

the second, and a singularity occurs for modes with nearly sonic phase speeds whenever N is greater than $1+M_1\cos\phi$. This condition means that if V, the flexural wave speed *in vacuo*, is faster than the sound speed in the moving fluid, or equivalently if the plate has a 'spring-like' response for modes with sonic phase speeds, the pressure spectrum is singular for spectral elements with phase speeds nearly equal to the sound speed. If, however, V is subsonic, (3.8) shows that the singularity occurs for spectral components with phase speeds nearly equal to V. These points are illustrated by the plots of D_{11} in figure 3. The graphs are for the case $M_1 = 0$. In figure 3(a) the bending wave speed V is subsonic, and, as predicted by the asymptotic theory for heavy plates, the pressure spectrum is finite for elements with sonic phase speeds, but it has a singularity for a particular spectral component whose phase speed is nearly equal to V. For the case illustrated in figure 3(b) the bending wave speed is supersonic, and then the pressure spectrum is finite for modes with phase speeds nearly equal to V, but is singular for nearly sonic modes. The values of N and $m\omega/\rho_0 c$ used in figures 3(a, b) correspond to a 5 cm thick steel plate in water at frequencies of 3 kHz and 6 kHz respectively.

3.3. *Sound-absorbing surfaces*

Flow over a sound-absorbing liner is known to influence its performance. An analysis of the effect of flow on liners in ducts is complicated by the duct modes (see Tester 1973a, b). But (2.23) can conveniently be used to determine the effect of flow and the surface properties on the simpler and analytically tractable problem of sound generated by turbulence near a plane sound absorber. The surface properties will be described in terms of an impedance $Z(\mathbf{k},\omega)$, where $Z(\mathbf{k},\omega)$ is the ratio of the surface-pressure perturbation to the normal surface velocity v_3 at wavenumber $\mathbf{k}$ and frequency ω; $Z(\mathbf{k},\omega) = -iX(\mathbf{k},\omega)/\omega$. $Z(\mathbf{k},\omega)$ relates the mean energy absorbed by unit area of the absorber in unit time to the surface pressure spectrum, since

$$\overline{(p-p_0)\,v_3} = \frac{1}{(2\pi)^3}\int \frac{P(\mathbf{k},\omega)}{Z(\mathbf{k},\omega)}\,d^2\mathbf{k}\,d\omega.$$

Since the surface absorbs energy, Re Z must be negative.

The predicted surface-pressure spectrum is equal to

$$D_{ij}D^{\dagger}_{kl}\rho_0^2 U_1^3 h^5 Q_{ijkl},$$

where D_{ij} is given by (2.22) with $X(\mathbf{k},\omega) = i\omega Z(\mathbf{k},\omega)$. Figure 4 shows plots of D_{11} for $Z(\mathbf{k},\omega) = -3\rho_0 c \mp 3i\rho_0 c$ with ω positive. The damping due to the energy absorbed by the surface ensures that all modes decay rapidly, and so there are no singularities in the surface-pressure spectrum. But, even so, some of the features observed in the case of the bending plate are still apparent. In figure 4(a), Im Z is positive and the surface has a 'spring-like' response, while in figure 4(b) Im Z is negative and the surface is 'mass-like'. A comparison of figures 4(a, b) shows that the pressure spectrum for spectral elements with sonic phase speeds is larger for a 'spring-like' surface than for a 'mass-like' surface. This is because for a 'spring-like' surface only damping prevents the pressure spectrum from being singular for these sonic spectral components, while for a 'mass-like' surface both the finite surface impedance and damping control the level of the pressure spectrum. It is apparent from figure 4 that a spring-like surface is more effective at absorbing the sound energy than a mass-like surface; and also that more sound energy propagating upstream is absorbed than that propagating downstream.

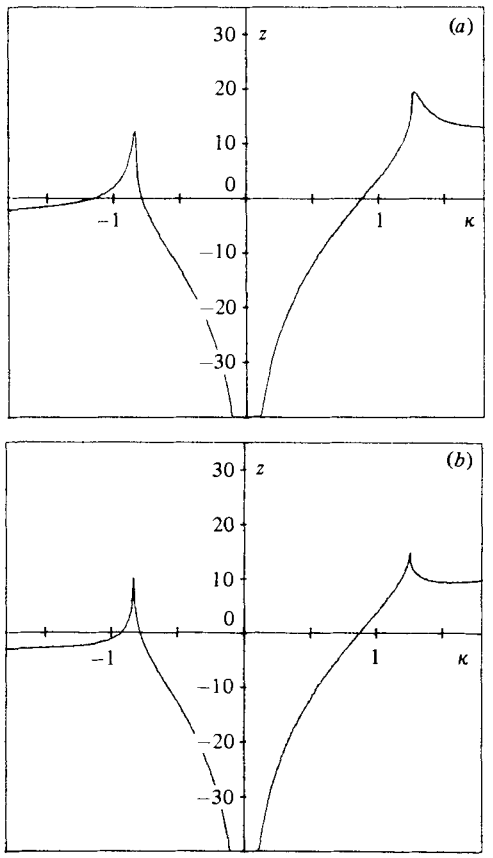

FIGURE 4. Plots of $z = 20\log_{10}|cD_{11}/\omega|$ *vs.* non-dimensional wavenumber $\kappa = k_1 c/\omega$ for a sound-absorbing surface with $k_2 = 0$, $M_1 = 0{\cdot}2$, $\omega h/c = 0{\cdot}1$, and (*a*) $Z = -3\rho_0 c + 3i\rho_0 c$, (*b*) $Z = -3\rho_0 c - 3i\rho_0 c$.

4. Conclusions

An analogy has been derived between the sound produced by turbulence in a boundary-layer flow and quadrupoles adjacent to a vortex sheet and a flexible boundary. The effect of the surface properties and mean flow on the sound field is brought out explicitly through the use of a Green function. This analogy has been used to derive a general expression for the low-wavenumber wall-pressure spectrum induced by a turbulent boundary layer over a surface. Although the analogy is always formally exact it is particularly relevant for these low-wavenumber spectral elements, because elements with wavelengths long in comparison with the boundary-layer scale are unable to detect the details of the velocity profile in the boundary layer. Hence a vortex-sheet analogy can be expected to demonstrate the essential structure of the low-wavenumber turbulent-pressure spectrum. The predicted pressure spectrum on a hard surface is found to be singular for spectral elements propagating downstream with an approximately sonic phase speed. This singularity is due to a trapped free mode of the system which propagates downstream supersonically within the stationary fluid in the boundary layer but is just subsonic in the moving stream. The next problem considered is that of a bending plate. It is found that plates in air are generally sufficiently massive compared with the effective fluid loading to behave like

a hard surface, but in underwater applications the pressure spectrum is dominated by the surface properties. In this limit V, the speed of flexural waves in the plate *in vacuo*, plays a crucial role in determining the form of the pressure spectrum on the plate. If V is subsonic, the predicted pressure spectrum has a double pole for spectral components whose phase speed is nearly equal to V, and the pressure spectrum remains finite for elements with sonic phase speeds. The position of the singularity is quite different when the flexural wave speed V is supersonic; then a singularity occurs in the pressure spectrum for spectral elements with sonic phase speeds. Finally, for the case of a surface covered by sound-absorbent material, both the mean flow and the surface properties affect the pressure spectrum. Investigation of the surface-pressure spectrum shows that a surface with a 'spring-like' response is more effective at absorbing the sound energy than one with a 'mass-like' response and the same damping.

It is a pleasure to thank Professor J. E. Ffowcs Williams and Dr I. Roebuck for their helpful suggestions and interest in this research. This work has been carried out with the support of the Procurement Executive, Ministry of Defence.

Appendix. The physical interpretation of G_0 and G_1

We define a direct Green function $G^{\mathrm{D}}(\mathbf{z}, s|\mathbf{y}, \tau)$. $G^{\mathrm{D}}(\mathbf{z}, s|\mathbf{y}, \tau)$ is to be the acoustic pressure disturbance at $(\mathbf{z}, s)$ due to a point source at $(\mathbf{y}, \tau)$ adjacent to a vortex sheet with mean position S_0 and a compliant boundary with mean position C_0. We can show that G^{D} and G are related.

G^{D} is a solution of

$$\left(\frac{\partial^2}{\partial s^2} - c^2\nabla^2\right) G_0^{\mathrm{D}} = \delta(\mathbf{z}-\mathbf{y}, s-\tau) \quad \text{in } V_0^0, \tag{A 1}$$

$$\left(\frac{\bar{D}^2}{Ds^2} - c^2\nabla^2\right) G_1^{\mathrm{D}} = \delta(\mathbf{z}-\mathbf{y}, s-\tau) \quad \text{in } V_1^0,$$

where V_0^0, V_1^0 are the initial regions within V_0 and V_1. G^{D} satisfies conditions of continuity of pressure and continuity of particle displacement across the vortex sheet S_0. These conditions can be written as

$$G_0^{\mathrm{D}} = G_1^{\mathrm{D}} \quad \text{on } S_0, \tag{A 2}$$

and ξ^{D}, the particle displacement caused by the point source, is continuous across S_0, where

$$\rho_0 \frac{\partial^2 \xi^{\mathrm{D}}}{\partial s^2} = -\frac{\partial G_0^{\mathrm{D}}}{\partial z_3}, \quad \rho_0 \frac{\bar{D}^2 \xi^{\mathrm{D}}}{Ds^2} = -\frac{\partial G_1^{\mathrm{D}}}{\partial z_3}. \tag{A 3}$$

G_0^{D} also satisfies the impedance condition

$$\overline{G_0^{\mathrm{D}}}(z_3, \mathbf{k}, \omega) = X(\mathbf{k}, \omega)\, \overline{\xi^{\mathrm{D}}}(\mathbf{k}, \omega) \quad \text{on } C_0. \tag{A 4}$$

Since C_0 is linearly disturbed from rest, the surface displacement ξ^{D} is related to G_0^{D} by

$$\rho_0 \frac{\partial^2 \xi^{\mathrm{D}}}{\partial s^2} = -\frac{\partial G_0^{\mathrm{D}}}{\partial z_3} \quad \text{on } C_0. \tag{A 5}$$

From the definition of the δ-function we can write

$$H_0 G_0^{\mathrm{D}}(\mathbf{x}, t|\mathbf{y}, \tau) = \int_\infty H_0 G_0^{\mathrm{D}}(\mathbf{z}, s|\mathbf{y}, \tau)\, \delta(\mathbf{z}-\mathbf{x}, t-s)\, d^3\mathbf{z}\, ds. \tag{A 6}$$

H_0 is a Heaviside function which is unity within V_0^0 and zero elsewhere. Using (2.8) we obtain

$$H_0 G_0^{\mathrm{D}}(\mathbf{x}, t|\mathbf{y}, \tau) = \int_{V_0^0} G_0^{\mathrm{D}} \left(\frac{\partial^2}{\partial s^2} - c^2\nabla^2\right) G_0(\mathbf{z}, s|\mathbf{x}, t)\, d^3\mathbf{z}\, ds$$

$$= \int_{V_0^0} G_0 \left(\frac{\partial^2}{\partial s^2} - c^2\nabla^2\right) G_0^{\mathrm{D}}(\mathbf{z}, s|\mathbf{x}, t)\, d^3\mathbf{z}\, ds$$

$$- c^2 \int_{S_0} \left(G_0^{\mathrm{D}} \frac{\partial G_0}{\partial z_3} - G_0 \frac{\partial G_0^{\mathrm{D}}}{\partial z_3}\right) dS\, ds + c^2 \int_{C_0} \left(G_0^{\mathrm{D}} \frac{\partial G_0}{\partial x_3} - G_0 \frac{\partial G_0^{\mathrm{D}}}{\partial z_3}\right) dS\, ds$$

after an application of Green's theorem. Finally we can use (A 1) and write

$$H_0 G_0^{\mathrm{D}}(\mathbf{x}, t|\mathbf{y}, \tau) = H_0 G_0(\mathbf{y}, \tau|\mathbf{x}, t) + c^2 \int_{C_0} \left(G_0^{\mathrm{D}} \frac{\partial G_0^{\mathrm{D}}}{\partial z_3} - G_0 \frac{\partial G_0^{\mathrm{D}}}{\partial z_3}\right) dS\, ds$$

$$- c^2 \int_{S_0} \left(G_0^{\mathrm{D}} \frac{\partial G_0}{\partial z_3} - G_0 \frac{\partial G_0^{\mathrm{D}}}{\partial z_3}\right) dS\, ds. \quad \text{(A 7)}$$

In a similar way we can show that

$$\bar{H}_0 G_1^{\mathrm{D}}(\mathbf{x}, t|\mathbf{y}, \tau) = \bar{H}_0 G_1(\mathbf{y}, \tau|\mathbf{x}, t) + c^2 \int \left(G_1^{\mathrm{D}} \frac{\partial G_1}{\partial z_3} - G_1 \frac{\partial G_1^{\mathrm{D}}}{\partial z_3}\right) dS\, ds. \quad \text{(A 8)}$$

The addition of (A 7) and (A 8) gives

$$H_0 G_0^{\mathrm{D}}(\mathbf{x}, t|\mathbf{y}, \tau) + \bar{H}_0 G_1^{\mathrm{D}}(\mathbf{x}, t|\mathbf{y}, \tau) = H_0 G_0(\mathbf{y}, \tau|\mathbf{x}, t) + \bar{H}_0 G_1(\mathbf{y}, \tau|\mathbf{x}, t) + \mathscr{C} + \mathscr{S}_1 - \mathscr{S}_0, \quad \text{(A 9)}$$

where

$$\mathscr{C} = c^2 \int_{C_0} \left(G_0^{\mathrm{D}} \frac{\partial G_0}{\partial z_3} - G_0 \frac{\partial G_0^{\mathrm{D}}}{\partial z_3}\right) dS\, ds,$$

$$\mathscr{S}_0 = c^2 \int_{S_0} \left(G_0^{\mathrm{D}} \frac{\partial G_0}{\partial z_3} - G_0 \frac{\partial G_0^{\mathrm{D}}}{\partial z_3}\right) dS\, ds,$$

$$\mathscr{S}_1 = c^2 \int_{S_0} \left(G_1^{\mathrm{D}} \frac{\partial G_1}{\partial z_3} - G_1 \frac{\partial G_1^{\mathrm{D}}}{\partial z_3}\right) dS\, ds.$$

Parseval's theorem enables $\mathscr{C}$ to be rewritten as

$$\mathscr{C} = \frac{c^2}{(2\pi)^3} \int \left\{\overline{G_0^{\mathrm{D}}}(0, \mathbf{k}, \omega) \overline{\frac{\partial G_0}{\partial z_3}}(0, -\mathbf{k}, -\omega) - \bar{G}_0(0, -\mathbf{k}, -\omega) \overline{\frac{\partial G_0^{\mathrm{D}}}{\partial z_3}}(0, \mathbf{k}, \omega)\right\} dk_1\, dk_2\, d\omega$$

$$= \frac{c^2}{(2\pi)^3} \int \left\{X(\mathbf{k}, \omega) \overline{\frac{\partial G_0}{\partial z_3}}(0, -\mathbf{k}, -\omega) - \omega^2 \rho_0 \bar{G}_0(0, -\mathbf{k}, -\omega)\right\} \bar{\xi}^{\mathrm{D}}(\mathbf{k}, \omega)\, dk_1\, dk_2\, d\omega,$$

from (A 4) and (A 5). The integral is identically zero because (2.11) shows that

$$\omega^2 \rho_0 \bar{G}_0(0, -\mathbf{k}, -\omega) = X(\mathbf{k}, \omega) \overline{\frac{\partial G_0}{\partial z_3}}(0, -\mathbf{k}, -\omega).$$

We can use the boundary conditions (2.10) and (A 3) to rewrite $\mathscr{S}_0$:

$$\mathscr{S}_0 = c^2 \int_{S_0} \left\{G_1^{\mathrm{D}} \frac{\partial G_1}{\partial z_3} + \rho_0 G_0 \frac{\partial^2 \xi^{\mathrm{D}}}{\partial s^2}\right\} dS\, ds$$

$$= c^2 \int_{S_0} \left\{G_1^{\mathrm{D}} \frac{\partial G_1}{\partial z_3} + \rho_0 \frac{\partial^2 G_0}{\partial s^2} \xi^{\mathrm{D}}\right\} dS\, ds,$$

by integration by parts. Then using (2.10) again

$$\mathscr{S}_0 = c^2 \int_{S_0} \left\{ G_1^{\mathrm{D}} \frac{\partial G_1}{\partial z_3} + \rho_0 \frac{\overline{D}^2 G_1}{Ds^2} \xi^{\mathrm{D}} \right\} dS\, ds$$

$$= c^2 \int \left\{ G_1^{\mathrm{D}} \frac{\partial G_1}{\partial z_3} + \rho_0 G_1 \frac{\overline{D}^2 \xi^{\mathrm{D}}}{Ds^2} \right\} dS\, ds,$$

after a further integration by parts. Finally ξ^{D} can be eliminated by the condition (A 3), and we find

$$\mathscr{S}_0 = c_0^2 \int_{S_0} \left\{ G_1^{\mathrm{D}} \frac{\partial G_1}{\partial z_3} - G_1 \frac{\partial G_1^{\mathrm{D}}}{\partial z_3} \right\} dS\, ds.$$

$$= \mathscr{S}_1.$$

The required reciprocal relationship follows from (A 9) as

$$H_0 G_0^{\mathrm{D}}(\mathbf{x}, t|\mathbf{y}, \tau) + \overline{H}_0 G_1^{\mathrm{D}}(\mathbf{x}, t|\mathbf{y}, \tau) = H_0 G_0(\mathbf{y}, \tau|\mathbf{x}, t) + \overline{H}_0 G_1(\mathbf{y}, \tau|\mathbf{x}, t). \qquad \text{(A 10)}$$

The Green function that appears in our analogy is therefore the response due to a point source adjacent to a vortex sheet and a compliant boundary. This is more general than the reciprocal relationship proved by Dowling *et al.* (1978). There the reciprocal Green function was only recognized as the vortex-sheet Green function in the far field. Equation (A 10) is, however, valid everywhere.

REFERENCES

Bergeron, R. F. 1973 *J. Acoust. Soc. Am.* **54**, 123–133.

Dowling, A. P., Ffowcs Williams, J. E. & Goldstein, M. E. 1978 *Phil. Trans. R. Soc. Lond.* A **288**, 321–349.

Ffowcs Williams, J. E. 1965 *J. Fluid Mech.* **22**, 507–519.

Ffowcs Williams, J. E. 1982 *J. Fluid Mech.* **125**, 9–25.

Ffowcs Williams, J. E. & Hawkings, D. L. 1969 *Phil. Trans. R. Soc. Lond.* A **264**, 321–342.

Ffowcs Williams, J. E. & Purshouse, M. 1981 *J. Fluid Mech.* **113**, 187–220.

Howe, M. S. 1979 *J. Sound Vib.* **65**, 159–164.

Jones, D. S. & Morgan, J. D. 1972 *Proc. Camb. Phil. Soc.* **72**, 465–488.

Lighthill, M. J. 1952 *Proc. R. Soc. Lond.* A **211**, 564–587.

Möhring, W. & Rahman, S. 1979 *J. Sound Vib.* **66**, 557–564.

Morse, P. M. & Feshbach, H. 1953 *Methods of Theoretical Physics.* McGraw-Hill.

Ross, D. 1976 *Mechanics of Underwater Noise*, pp. 184–196. Pergamon.

Tester, B. J. 1973*a* *J. Sound Vib.* **28**, 151–203.

Tester, B. J. 1973*b* *J. Sound Vib.* **28**, 217–245.

Willmarth, W. W. 1975 *Ann. Rev. Fluid Mech.* **7**, 13–38.